Probing the Micellization Kinetics of Pyrene End-Labeled Diblock Copolymer via a Combination of Stopped-Flow Light-Scattering and Fluorescence Techniques

Jingyan Zhang,[†,‡] Yuting Li,[§] Steven P. Armes,[§] and Shiyong Liu*[,†]

Department of Polymer Science and Engineering, Joint Laboratory of Polymer Thin Films and Solution, Hefei National Laboratory for Physical Sciences at the Microscale, University of Science and Technology of China, Hefei, Anhui 230026, China; School of Materials and Chemical Engineering, Anhui Institute of Architecture and Industry, Hefei, Anhui 230022, China; and Department of Chemistry, University of Sheffield, Brook Hill, Sheffield, South Yorkshire, S37HF United Kingdom

Received: June 27, 2007; In Final Form: August 25, 2007

A pyrene end-labeled double hydrophilic diblock copolymer, poly(2-(diethylamino)ethyl methacrylate)-*b*-poly(2-(dimethylamino)ethyl methacrylate) (*Py*-PDEA-*b*-PDMA), was synthesized by sequential monomer addition via oxyanionic polymerization using a 1-pyrenemethanol-based initiator. This diblock copolymer exhibits reversible pH-responsive micellization behavior in aqueous solution, forming PDEA-core micelles stabilized by the soluble PDMA block at neutral or alkaline pH. Taking advantage of the pyrene probe covalently attached to the end of the PDEA block, the pH-induced micellization kinetics of *Py*-PDEA-*b*-PDMA was monitored by stopped-flow light scattering using a fluorescence detector. Upon a pH jump from 4.0 to 9.0, both the scattered light intensity and excimer/monomer fluorescence intensity ratios (I_E/I_M) increase abruptly initially, followed by a more gradual increase to reach plateau values. Interestingly, the I_E/I_M ratio increases abruptly within the first 10 ms: a triple exponential function is needed to fit the corresponding dynamic trace, leading to three characteristic relaxation time constants ($\tau_{1,fluo} < \tau_{2,fluo} < \tau_{3,fluo}$). On the other hand, dynamic traces for the scattered light intensity can be well-fitted by double exponential functions: the resulting time constants $\tau_{1,scat}$ and $\tau_{2,scat}$ can be ascribed to formation of the quasi-equilibrium micelles and relaxation into their final equilibrium state, respectively. Most importantly, $\tau_{1,scat}$ obtained from stopped-flow light scattering is in general agreement with $\tau_{2,fluo}$ obtained from stopped-flow fluorescence. The fastest process ($\tau_{1,fluo} \sim 4$ ms) detected by stopped-flow fluorescence is ascribed to the burst formation of small transient micelles comprising only a few chains, which are too small to be detected by conventional light scattering. These nascent micelles undergo rapid fusion and grow into quasi-equilibrium micelles and then slowly approach their final equilibrium state. The latter two processes can be detected by both techniques.

Introduction

Because of their promising applications in diverse fields such as drug delivery, gene therapy, interface mediators, biosensing, soft actuators/valves, and catalysis, double hydrophilic block copolymers (DHBCs) have received increasing attention.[1−13] When subjected to physical or chemical transformations in aqueous solution, one of the blocks of DHBCs can be selectively rendered water-insoluble, while the other block still remains well-solvated to stabilize the formed colloidal aggregates. Under appropriate conditions (e.g., pH, temperature, and ionic strength), certain DHBCs can even self-assemble into one or more types of micellar aggregates, that is, they exhibit so-called "schizophrenic" micellization behavior.[6,14−31]

Since pH changes can be exploited both in vitro and in vivo,[32] a wide range of pH-responsive DHBCs containing ionizable blocks with tunable water solubility, such as poly(methacrylic acid), poly(2-(diethylamino)ethyl methacrylate) (PDEA),[27,33] poly(vinyl pyridine) (PVP),[34] and poly(4-vinylbenzoic acid) (PVBA),[6] have been extensively studied. The first example of pH-induced micellization of DHBCs was reported by Martin et al. Poly(ethylene oxide)-*b*-poly(2-vinyl pyridine) (PEO-*b*-P2VP) is molecularly soluble in acidic pH but forms near-monodisperse P2VP-core micelles above the pK_a of the P2VP block because of its deprotonation.[35] Armes and co-workers then reported more sophisticated examples of PDEA-containing DHBCs, which can self-assemble into two types of structurally "inverted" micelles in aqueous solution by solely manipulating the solution pH or by a judicious combination of pH and temperature stimuli.[36−45]

However, most previous studies concerning DHBCs focused on the characterization of their equilibrium self-assembled structures by laser light scattering (LLS), small-angle neutron scattering (SANS), ^{1}H NMR, and transmission electron microscopy.[6,14−27,46,47] On the other hand, the kinetics of micellar self-assembly of DHBCs is of fundamental interest, since it is important for various technological processes such as foaming, wetting, emulsification, solubilization, and detergency.

Theoretically, Halperin and Alexander considered the characteristic relaxation time required for a copolymer chain to escape from a micelle on the basis of scaling analysis within the context of the Aniansson and Wall (A-W) theory for small molecule surfactants.[48] They concluded that the insertion/expulsion of individual chains (unimer exchange) is the only

* To whom correspondence should be addressed. E-mail: sliu@ustc.edu.cn.
† University of Science and Technology of China.
‡ Anhui Institute of Architecture and Industry.
§ University of Sheffield.

10.1021/jp075018b CCC: $37.00
Published on Web 10/05/2007

mechanism for micelle relaxation processes for small perturbations from the equilibrium state.

For large deviations from the initial state, such as a unimer-to-micelle transition, computer simulations performed by Wang et al.[49] suggested two processes operating on different time scales: the volume fraction of free chains reaches its equilibrium value very quickly in the initial fast step followed by a step toward the equilibrium state at a much slower rate. Dormidontova and co-workers[50−52] further proposed a micelle fusion/fission−unimer expulsion/entry joint mechanism for block copolymer micelle evolution. It was suggested that micelle fusion/fission dominates over unimer entry/expulsion in the initial fast process while a unimer entry/expulsion mechanism dominates during the second slow process. However, Nrykova and Semenov[53,54] recently postulated that the unimer−micelle transition cannot be simply characterized by just two relaxation times but rather by a continuous spectrum of relaxation times. They also proposed that the main route of micelle growth should involve step-by-step sequential aggregation of unimers, that is, insertion/expulsion of individual chains. Thus, a theoretical consensus concerning the detailed nature of the kinetics of micellization has not been reached.

Recently, we reported the kinetics of pH-induced micellization of a stimulus-responsive ABC triblock copolymer, namely, poly(glycerol monomethacrylate)-*b*-poly(2-(dimethylamino)ethyl methacrylate)-*b*-poly(2-(diethylamino)ethyl methacrylate) (PGMA-*b*-PDMA-*b*-PDEA).[55] The micellization kinetics was investigated by stopped-flow light scattering and was analyzed in the context of the Dormidontova theory. Upon jumping from pH 4 to 12, the early stages of micellization occurred via two successive processes. The initial fast process (τ_1) is associated with the formation of quasi-equilibrium micelles, and the subsequent slow process (τ_2) is attributed to micelle formation and breakup, approaching the final equilibrium state. τ_2 is almost independent of the copolymer concentration, indicating that the slow process proceeds mainly via the unimer insertion/expulsion mechanism. We also studied the micellar formation and inversion kinetics of a schizophrenic diblock copolymer of poly(4-vinylbenzoic acid)-*b*-poly(*N*-(morpholino)ethyl methacrylate) (VBA-*b*-MEMA) induced by variation of both the solution pH and the ionic strength.[56]

The change in scattered light intensity at a scattering angle of 90° mainly reflects the evolution of the mean aggregation number (N_{agg}) per micelle during micellization. For minimal variation of N_{agg} from the unimer state, that is, in the early stages of micellization, the change in scattered light intensity is not sufficiently sensitive. Previously, the fast relaxation process (τ_1) was ascribed to the formation of quasi-equilibrium micelles. Theoretically, this process will proceed first with the formation of a large number of small transient micelles, and the unimer concentration is simultaneously reduced to close to the critical micellization concentration (cmc); these small transient micelles then grow and fuse into quasi-equilibrium micelles. However, stopped-flow light scattering cannot differentiate between these subprocesses. On the other hand, during the second slow process (τ_2), some structural rearrangement of chain segments within the micelle core or corona may well occur, but such subtleties are beyond the scope of the stopped-flow light-scattering technique.

Fluorescence spectroscopy is well-known for its extremely high sensitivity compared to that of LLS. Pyrene has been widely used as a probe of polymer structure and dynamics because of its long-lived excited state and spectral sensitivity to the surrounding medium.[57,58] Fluorescence measurements of the excimer-to-monomer intensity ratio (I_E/I_M) provide highly localized information, because the excimer is only formed when aromatic rings closely approach each other within 4−5 Å, that is, they are quite sensitive to the formation of small aggregates containing two or more pyrene groups and their compactness, with the latter determining the mobility of pyrene groups and their encounter probability.[59−68] Thus, the combination of stopped-flow light-scattering and fluorescence studies of pyrene-labeled DHBCs should be able to further elucidate the kinetics and detailed mechanism of the micellar self-assembly of DHBCs in aqueous solution.

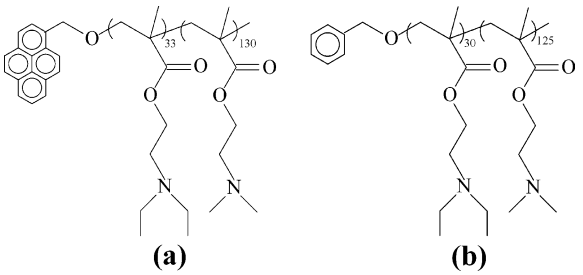

Figure 1. Chemical structures of the pH-responsive (a) *Py*-PDEA-*b*-PDMA and (b) label-free PDEA-*b*-PDMA double hydrophilic diblock copolymers used in this study.

Herein, we synthesized a pyrene end-labeled double hydrophilic block copolymer, poly(2-(diethylamino)ethyl methacrylate)-*b*-poly(2-(dimethylamino)ethyl methacrylate) (*Py*-PDEA-*b*-PDMA), by oxyanionic polymerization using sequential monomer addition. The general micellization behavior of such PDEA-*b*-PDMA block copolymers has been reported by Armes and co-workers.[36,39,40,42,43,69] This type of diblock copolymer is molecularly soluble in acidic pH but undergoes reversible pH-induced micellization in aqueous solution forming PDEA-core micelles stabilized by the soluble PDMA block at neutral or alkaline pH. We studied the pH-induced micellization kinetics of *Py*-PDEA-*b*-PDMA by a combination of stopped-flow light-scattering and fluorescence techniques. For the first time, we were able to detect the formation of small transient micelles by stopped-flow fluorescence. During the subsequent slow rate of micelle formation/breakup, unambiguous evidence for the structural rearrangement of PDEA chains was obtained by comparing the stopped-flow light-scattering and fluorescence data.

Experimental Section

Materials. 1-Pyrenemethanol, 2-(dimethylamino)ethyl methacrylate (DMA), 2-(diethylamino)ethyl methacrylate (DEA), and potassium *tert*-butoxide (1.0 M in THF) were all purchased from Aldrich. Both monomers were passed through basic alumina columns, were stirred over calcium hydride for 24 h, were stored at −20 °C, and were distilled immediately prior to use. THF was dried with sodium wire for 3 days and was subsequently refluxed in the presence of potassium. It was distilled under nitrogen just prior to use. All glassware was heated overnight at 150 °C before use. Assembled glassware was then flamed under vacuum to eliminate the surface moisture. Liquid reagents were handled using standard Schlenk techniques.[45,69]

Synthesis of *Py*-PDEA-*b*-PDMA. The chemical structures of the *Py*-PDEA-*b*-PDMA and label-free PDEA-*b*-PDMA diblock copolymers are shown in Figure 1. It was synthesized by oxyanionic polymerization using sequential monomer addition via the following protocol. The glassware and experimental setup were described above. 1-Pyrenemethanol (0.58 g, 2.5 mmol) was added as a solid through a sidearm of the polym-

erization flask. To this flask was added anhydrous THF (250 mL) via a double-tipped needle. To this solution was added potassium *tert*-butoxide (2.5 mL, 1.0 M in THF), and the reaction mixture was stirred for approximately 30 min at 50 °C. Subsequently, freshly distilled DEA (15.0 mL, 13.8 g, 74.6 mmol, target DP = 30) was added dropwise to the reaction flask, and polymerization was initiated by the in-situ generated potassium 1-pyrenemethoxide initiator. After 20 min, freshly distilled DMA (52.5 mL, 49.0 g, 0.312 mol, target DP = 125) was added dropwise to the living PDEA solution at 50 °C. After 2 h, the polymerization was terminated with degassed methanol. The reaction mixture was passed through a silica column and THF was removed under reduced pressure; the obtained solid was washed three times with *n*-hexane to remove traces of unreacted initiator and also any PDEA homopolymer contamination. Finally, the purified copolymer was dried in a vacuum oven overnight at room temperature. The overall yield of the isolated, purified *Py*-PDEA-*b*-PDMA was 72%.

The mean degrees of polymerization (DPs) of each block were determined using ^{1}H NMR spectroscopy in $CDCl_3$ and were found to be 33 and 130 for the PDEA and PDMA blocks, respectively. Thus, the diblock copolymer was denoted *Py*-$PDEA_{33}$-*b*-$PDMA_{130}$. These DP values are in general agreement with those originally targeted. The polydispersity, M_w/M_n, was estimated to be 1.27 by gel permeation chromatography (GPC) using THF eluent and poly(methyl methacrylate) calibration standards (PLgel 3 μm MIXED-E 300 × 7.5 μm column, refractive index detector).[45,69] For comparison, label-free $PDEA_{30}$-*b*-$PDMA_{125}$ diblock copolymer was also prepared following similar procedures as described above except that benzyl alcohol-based initiator was used as the initiator.

Characterization. *Nuclear Magnetic Resonance (NMR) Spectroscopy.* All ^{1}H NMR spectra performed at 25 °C on a Bruker AV300 NMR spectrometer (resonance frequency of 300 MHz for ^{1}H) operating in the Fourier transform mode.

Potentiometric Titrations. The *Py*-PDEA-*b*-PDMA diblock copolymer was first dissolved in deionized water that had been adjusted to pH 2 using HCl. This copolymer solution was then titrated by the dropwise addition of dilute NaOH (pH 12.4), and the solution pH was monitored with a Corning Check-Mite pH meter (precalibrated with pH 4.0, 7.0, and 10.0 buffer solutions).

Dynamic Laser Light Scattering (DLS). A commercial spectrometer (ALV/DLS/SLS-5022F) equipped with a multi-tau digital time correlator (ALV5000) and a cylindrical 22 mW UNIPHASE He−Ne laser (λ_0 = 632 nm) as the light source was employed for dynamic LLS measurements. The intensity-average hydrodynamic radius, $\langle R_h \rangle$, and polydispersity of the micelles were obtained by cumulants analysis of the experimental correlation function.

Fluorescence Spectroscopy. Fluorescence spectra were recorded using a Shimadzu RF-5301PC spectrofluorimeter. The temperature of the water-jacketed cell holder was controlled at 25 °C by a programmable circulation bath. The excitation wavelength was set at 330 nm with the excitation and emission slit widths both adjusted to 10.0 nm. The excimer-to-monomer ratio was calculated from the ratio of the emission intensity at 480 nm to that of the emission at 370 nm.

Stopped-Flow Light Scattering and Fluorescence. Stopped-flow studies were carried out using a Bio-Logic SFM300/S stopped-flow instrument.[55,70] The SFM-300/S is a three-syringe (10 mL) instrument in which all three stepper motor-driven syringes (S1, S2, S3) can be operated independently for either single or double mixing. The SFM-300/S stopped-flow device is attached to the MOS-250 spectrometer through optical fiber connection. Thirty shots were conducted successively for each mixing ratio and an average dynamic curve was obtained with kinetic data being fitted using the Biokine program (Bio-Logic). For the detection of light-scattering intensity, both the excitation and emission wavelengths were adjusted to 330 nm. For fluorescence detection, the excitation wavelength was set at 338 nm, and the emission wavelengths were, respectively, set at 370 and 480 nm to record the time dependence of the respective intensities because of the monomer and excimer fluorescence. Five nanometer slits were always used for both the excitation and emission monochromator. The typical dead times for the FC-08 or FC-15 stopped-flow cells were about 1.1 and 2.6 ms, respectively. Temperature was maintained at 25 °C by circulating water around the syringe chamber and observation head.

Results and Discussion

Micellization of *Py*-PDEA-*b*-PDMA. Both PDMA and PDEA are weak polybases with conjugate acid pK_a values of 7.0 and 7.3, respectively.[38,39,42,43,71] PDMA homopolymer is water-soluble over the whole pH range but becomes significantly less hydrophilic in its neutral form above pH 9−10. In contrast, PDEA homopolymer is water-insoluble at neutral or alkaline pH. Below pH 6, both PDMA and PDEA are soluble as weak cationic polyelectrolytes because of protonation of their tertiary amine groups. The micellization behavior of PDEA-*b*-PDMA block copolymers has been extensively studied by Armes and co-workers.[36−45,69] PDEA-*b*-PDMA dissolves molecularly in acidic media but forms micelles above pH 7−8 with hydrophobic PDEA cores and almost neutral (or only weakly cationic) PDMA coronas because of deprotonation of both blocks.

Figure 2a shows the titration curve obtained for *Py*-$PDEA_{33}$-*b*-$PDMA_{130}$. As the conjugate acid forms of both blocks possess similar pK_a values, this titration curve is quite similar to that of PDMA or PDEA homopolymer.[43] The diblock copolymer buffers the solution from pH 6 to pH 8. From Figure 2b, we can see that the overall degree of protonation (α) of the tertiary amine residues decreases from unity to zero as the solution pH increases from 4.3 to 9.1. However, within this pH range, the PDMA block is presumably slightly more deprotonated than the PDEA block because of the former block's lower basicity. The overall pK_a of the *Py*-$PDEA_{33}$-*b*-$PDMA_{130}$ was determined to be 6.7 at α = 0.5, which is slightly lower than that of the PDMA and PDEA homopolymers. In this context, we note that Plamper et al.[72] synthesized star-shaped poly(acrylic acid) and found that the apparent pK_a values increase with increasing arm number because of increasing segment density.

Acid−base titration of label-free $PDEA_{30}$-*b*-$PDMA_{125}$ diblock copolymer (Figure 2a inset and Figure 2b) indicates that deprotonation occurs in the pH range of 4.5−9.2 with an overall pK_a of 6.8, which is quite comparable to that of *Py*-$PDEA_{33}$-*b*-$PDMA_{130}$. This suggests that the presence of hydrophobic pyrene terminal group in *Py*-$PDEA_{33}$-*b*- $PDMA_{130}$ exhibits no appreciable effects on the pK_a as compared to that of label-free ones.

Vamvakaki et al.[73] studied the pH-responsive micellization of poly(hexa(ethylene glycol) methacrylate)-*b*-poly(2-(diethylamino)ethyl methacrylate) (PHEGMA-*b*-PDEA) and determined the critical degree of protonation required to induce the formation of PDEA-core micelles via a combination of dynamic LLS and ^{1}H NMR. At $\alpha \geq 0.3$, the copolymer chains remained as unimers; at α = 0.2, some aggregates with an average hydrodynamic radius, $\langle R_h \rangle$, of a few tens of nanometers were formed; at α = 0.1, hydrated micelles began to form; however,

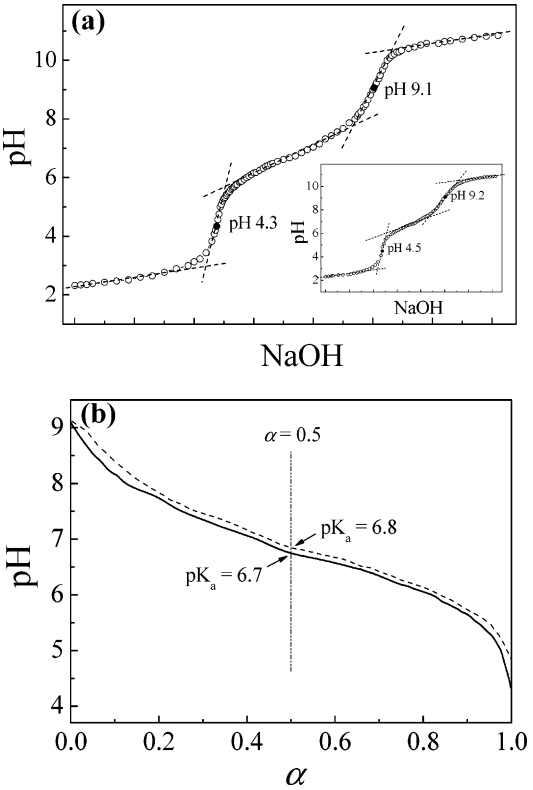

Figure 2. (a) Acid titration curve obtained for a 1.0 g/L aqueous solution of *Py*-PDEA$_{33}$-*b*-PDMA$_{130}$ diblock copolymer. The inset shows the titration curve of label-free PDEA$_{30}$-*b*-PDMA$_{125}$ diblock copolymer. (b) Same titration curves of aqueous solutions of *Py*-PDEA$_{33}$-*b*-PDMA$_{130}$ (solid line) and label-free PDEA$_{30}$-*b*-PDMA$_{125}$ (dashed line) diblock copolymers as in a with the *x*-axis expressed in terms of the mean degree of protonation, α.

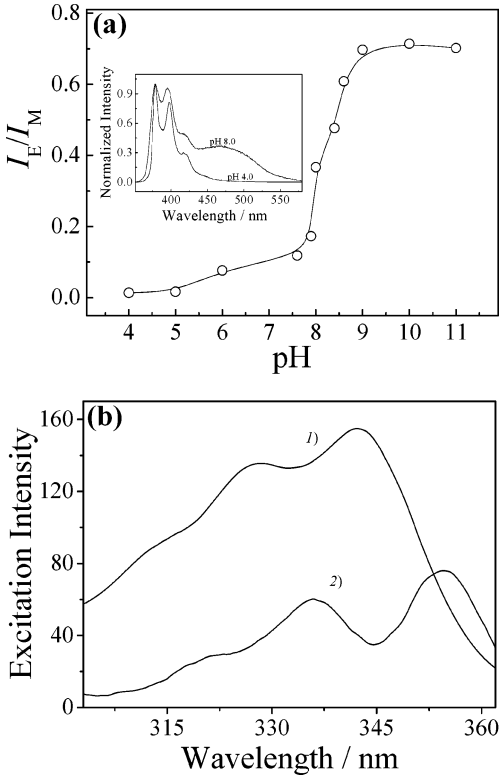

Figure 3. (a) pH dependence of the excimer/monomer (I_E/I_M) ratio calculated from the fluorescence emission intensities obtained for a 1.0 g/L aqueous solution of *Py*-PDEA-*b*-PDMA. The inset shows typical normalized fluorescence emission spectra recorded for the same *Py*-PDEA-*b*-PDMA aqueous solution at pH 4.0 and pH 8.0. (b) Excitation fluorescence spectra of a 1.0 g/L aqueous solution of *Py*-PDEA-*b*-PDMA at pH 6.9 monitored (1) at the monomer wavelength (370 nm) and (2) at the excimer wavelength (480 nm).

only after complete deprotonation of the PDEA block (α = 0) were equilibrium micelles finally formed.

If we assume that the pH dependence of the degree of protonation α of the diblock copolymer also reflects that of the core-forming PDEA block, we deduce from Figure 2b that the *Py*-PDEA$_{33}$-*b*-PDMA$_{130}$ copolymer should molecularly dissolve below pH 7.3 and form interchain aggregates, hydrated micelles, and equilibrium micelles above pH 7.6, 8.3, and 9.0, respectively. However, the pH dependence of α in the current study might not be the same as those of PHEGMA-*b*-PDEA.[73] Moreover, the actual aggregation and micellization behavior of *Py*-PDEA$_{33}$-*b*-PDMA$_{130}$ will be further complicated by the presence of the terminal hydrophobic pyrene group, which will be discussed below.

The critical pH of 9.0 required for the formation of fully hydrophobic PDEA-core micelles should be accurate because deprotonation of the PDEA block occurs slightly more readily than that of the PDMA block. Indeed, a typical bluish tinge that is characteristic of micellar solutions is observed at pH > 9. Dynamic LLS measurements of the *Py*-PDEA$_{33}$-*b*-PDMA$_{130}$ copolymer in aqueous solution at pH 9.0 and a concentration of 1.0 g/L revealed the presence of relatively monodisperse PDEA-core micelles with an average hydrodynamic radius, $\langle R_h \rangle$, of 21 nm, and a polydispersity, μ_2/Γ^2, of 0.11. As the PDEA block gets completely deprotonated at pH 9.0, these micelles possess fully hydrophobic cores stabilized by neutral PDMA coronas. Moreover, the sizes of PDEA-core micelles formed at pH 9.0 are almost independent of polymer concentrations in the range of 0.3−1.0 g/L. This indicates that in this concentration range, only the number density of micelles changes with polymer concentrations.

Figure 3a shows typical fluorescence emission spectra of *Py*-PDEA$_{33}$-*b*-PDMA$_{130}$ recorded at different pH's and the variation in I_E/I_M as a function of solution pH. No excimer peak is detected at pH 4.0, which indicates that the diblock copolymer dissolves molecularly in acidic solution with spatially isolated pyrene end groups. Upon increasing the solution pH to 8.0, pyrene excimer emission produces a broad, featureless band at around 480 nm. This suggests the formation of PDEA-core micelles with localization of the terminal pyrene groups within the micelle core, and the much closer proximity of the pyrene groups leads to more efficient energy exchange between them. Of particular interest is I_E/I_M (arising from the excimer and monomer signals at 480 and 370 nm, respectively), which is directly related to the efficiency of excimer formation. At pH 4−5, this I_E/I_M ratio is close to zero. Increasing the solution pH up to 6−7.6 slightly increases the I_E/I_M ratio for *Py*-PDEA$_{33}$-*b*-PDMA$_{130}$. On the basis of the titration data (Figure 2), the degree of protonation (α) of the PDEA block should be more than 20% within this pH range. On the basis of fluorescence emission spectra of *Py*-PDEA$_{33}$-*b*-PDMA$_{130}$ recorded at different pH's, we conclude that the appearance of a weak excimer emission peak between pH 6 and pH 7.6 is due to the hydrophobic association of pyrene end groups.[62,65] Such interactions lead to formation of loose interchain aggregates.

The presence of these interchain aggregates was further confirmed by examining the respective excitation spectra monitored at the monomer and excimer wavelengths (Figure 3b). Clearly, the two excitation spectra recorded at pH 6.9 do not coincide: a red shift of ∼10 nm is observed. This indicates the presence of pyrene dimers within the interchain aggregates

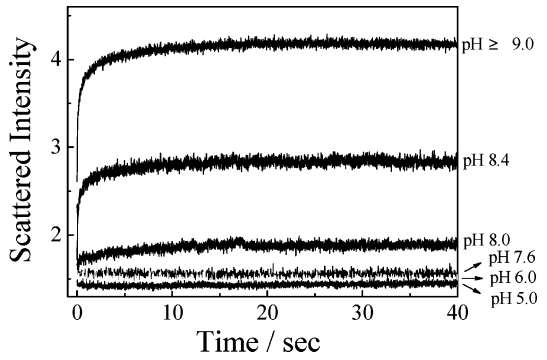

Figure 4. Time dependence of the scattered light intensity for aqueous solutions of *Py*-PDEA-*b*-PDMA after a pH jump from 4.0 to various final pH values. The final copolymer concentration was fixed at 1.0 g/L.

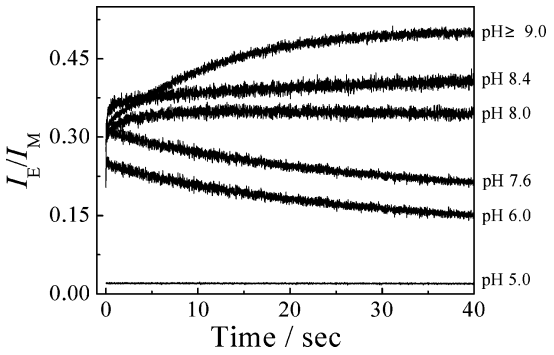

Figure 5. Time dependence of the excimer/monomer (I_E/I_M) ratio calculated from the fluorescence emission intensities recorded for an aqueous solution of *Py*-PDEA-*b*-PDMA after a pH jump from 4.0 to various final pH values. The final copolymer concentration was fixed at 1.0 g/L.

because of hydrophobic associations between pyrene groups.[74,75] In contrast, the label-free $PDEA_{30}$-*b*-$PDMA_{125}$ diblock copolymer is molecularly dissolved. No excimer peak was observed at pH 4−5 suggesting no hydrophobic association between pyrene groups occurs under these conditions. This is understandable since both the PDMA and PDEA blocks are fully protonated, and hence mutually repulsive, in such acidic media.

Above pH 8, an abrupt increase of I_E/I_M is observed, indicating the initial formation of hydrated micelles. Above pH 9, the I_E/I_M value reaches a plateau, and micelles with fully hydrophobic PDEA cores are formed. This is in agreement with the titration results (Figure 2) and also data reported by Vamvakaki et al.[73]

Stopped-Flow Kinetics. Figures 4 and 5 depict the time dependence for the scattered light intensity and the excimer/monomer (I_E/I_M) ratio after jumping from pH 4.0 to different final pH values. On jumping from pH 4.0 to pH 5.0, the dynamic traces obtained for both parameters remained flat and no relaxation processes were observed. At pH 5, almost all the amine residues were protonated (Figure 2b), the copolymer chains remained molecularly dissolved, and no interchain aggregates were formed because of hydrophobic association between pyrene groups, as indicated by the absence of an excimer emission peak (Figure 3a). On jumping from pH 4.0 to a final pH of 6.0−7.6, the dynamic traces obtained for the scattered light intensity still exhibited no apparent relaxation processes, but the I_E/I_M ratio, which is much larger than that at pH 4−5 just after mixing, decreased continuously with time. As discussed previously, the label-free $PDEA_{30}$-*b*-$PDMA_{125}$ diblock copolymer molecularly dissolves at pH 6.0 and forms ill-defined interchain aggregates at pH 7.6. For *Py*-$PDEA_{33}$-*b*-$PDMA_{130}$, static fluorescence emission spectra already revealed the presence of an excimer signal because of the hydrophobic association of pyrene groups. On jumping from pH 4.0 to pH 6.0−7.6, rapid association of hydrophobic pyrene groups occurred within the stopped-flow dead time (2−3 ms), and the subsequent monotonic reduction of I_E/I_M with time suggests slow structural evolution of these loose interchain aggregates. As the scattered light intensity does not reveal any further changes compared to that observed at pH 4−5, we conclude that these interchain aggregates comprise only a few chains. This difference indicates that scattered light intensity are insensitive to small changes in N_{agg} as expected.

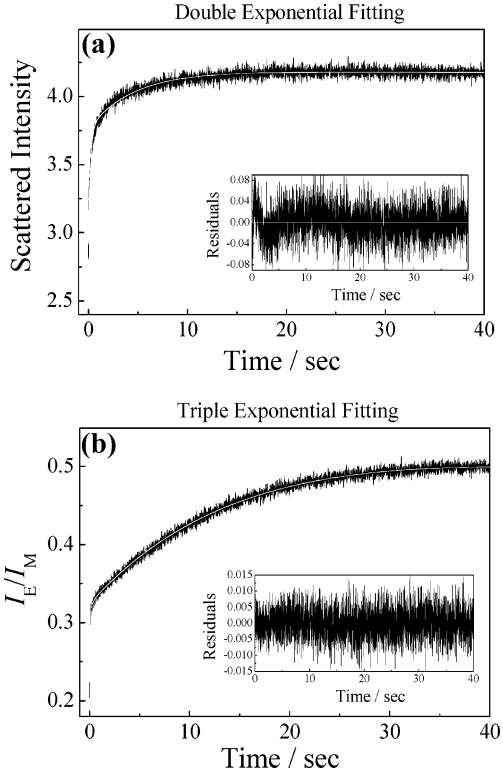

Figure 6. Typical time dependence of (a) the scattered light intensity and (b) the excimer/monomer (I_E/I_M) ratio recorded for an aqueous solution of *Py*-PDEA-*b*-PDMA during the micellar self-assembly induced by a pH jump from 4.0 to 9.0. The upper and lower plots were fitted by double and triple exponential functions (gray line), respectively. The final copolymer concentration was fixed at 1.0 g/L.

In contrast, if the final pH ≥ 8.0, stopped-flow pH jump studies confirmed that both the scattered light intensity and the I_E/I_M ratio increase with time (Figures 4−5). This is consistent with the formation of hydrated micelles. As discussed previously, at a final pH ≥ 9.0, all the tertiary amine groups in *Py*-$PDEA_{33}$-*b*-$PDMA_{130}$ are deprotonated and micelles with fully hydrophobic PDEA cores are formed. Dynamic traces recorded for the scattered light intensity and I_E/I_M are co-incident if the final pH is larger than 9.0, indicating that PDEA-core micelles with equilibrium structures are formed.

Closer examination of the dynamic traces because of the scattered light intensity and the I_E/I_M ratio at a final pH ≥ 9.0 confirmed that they report differing kinetic information. Initially, the scattered light intensity abruptly increases with time and then gradually stabilizes after ∼10−20 s. However, the I_E/I_M ratio exhibits a sudden increase within 10 ms of the pH jump followed by a gradual increase prior to attaining a plateau value at extended times (∼30 s). Typical fits for the time dependence of the scattered light intensity and the I_E/I_M ratio for a pH jump from 4.0 to ≥9.0 are shown in Figure 6.

TABLE 1: Summary of the Data Calculated from Double- and Triple-Exponential Fits to the Dynamic Traces Shown in Figure 6[a]

scattered intensities				
$c_{1,scat}$	$c_{2,scat}$		$\tau_{1,scat}$/S	$\tau_{2,scat}$/S
0.65	0.35		0.21	4.5

I_E/I_M					
$c_{1,fluo}$	$c_{2,fluo}$	$c_{3,fluo}$	$\tau_{1,fluo}$/S	$\tau_{2,fluo}$/S	$\tau_{3,fluo}$/S
0.28	0.05	0.67	0.004	0.19	13.7

[a] τ_i, characteristic relaxation time; c_i, amplitudes associated with τ_i. The accuracy of the obtained τ_i and c_i values was within ±5%.

The time dependence of the scattered light intensity, I_t, can be converted to a normalized function, namely, $(I_\infty - I_t)/I_\infty$ versus t, where I_∞ is the value of I_t at an infinitely long time. Like the traces reported previously for the pH-induced micellization kinetics of PGMA-*b*-PDMA-*b*-PDEA,[55] these dynamic traces can be well-fitted by the following double exponential function (Figure 6a)

$$(I_\infty - I_t)/I_\infty = c_1 e^{-t/\tau_1} + c_2 e^{-t/\tau_2} \quad (1)$$

where c_1 and c_2 are the normalized amplitudes ($c_2 = 1 - c_1$), τ_1 and τ_2 are the characteristic relaxation times for two processes, $\tau_1 < \tau_2$, and they are denoted $c_{1,scat}$, $c_{2,scat}$, $\tau_{1,scat}$, and $\tau_{2,scat}$. The mean relaxation time for the overall micelle formation, $\tau_{f,scat}$, can be calculated as

$$\tau_{f,scat} = c_{1,scat}\tau_{1,scat} + c_{2,scat}\tau_{2,scat} \quad (2)$$

Both processes associated with $\tau_{1,scat}$ and $\tau_{2,scat}$ have positive amplitudes. For a pH jump from 4.0 to a final pH ≥ 9.0 at a copolymer concentration of 1.0 g/L, $\tau_{1,scat}$ and $\tau_{2,scat}$ are approximately 0.21 ± 0.01 s and 4.5 ± 0.2 s, respectively.

The evolution of the I_E/I_M ratio exhibits qualitatively different kinetic behavior compared to that observed for the scattered light intensity; the former experiences a sudden increase within the initial 10 ms (Figure 6b). Although double exponential functions cannot fit this time dependence, the dynamic trace of I_E/I_M could be well-fitted by a triple exponential function of the form

$$(I_\infty - I_t)/I_\infty = c_1 e^{-t/\tau_1} + c_2 e^{-t/\tau_2} + c_3 e^{-t/\tau_3} \quad (3)$$

where c_1, c_2, and c_3 are the normalized amplitudes, and τ_1, τ_2, and τ_3 are the characteristic relaxation times for three processes, denoted $c_{1,fluo}$, $c_{2,fluo}$, $c_{3,fluo}$, $\tau_{1,fluo}$, $\tau_{2,fluo}$, and $\tau_{3,fluo}$, respectively (such that $\tau_{1,fluo} < \tau_{2,fluo} < \tau_{3,fluo}$). For the pH jump from 4.0 to a final pH ≥ 9.0, $\tau_{1,fluo}$,$\tau_{2,fluo}$, and $\tau_{3,fluo}$ are 0.004 ± 0.0002 s, 0.19 ± 0.01 s, and 13.7 ± 0.7 s, respectively.

The results obtained from fitting the dynamic traces of the scattered light intensity and the I_E/I_M ratio are summarized in Table 1. $\tau_{1,scat}$ obtained from stopped-flow light scattering was in general agreement with $\tau_{2,fluo}$ value obtained from stopped-flow fluorescence, suggesting that $\tau_{2,fluo}$ can be ascribed to similar processes as those of $\tau_{1,scat}$. The fast process ($\tau_{1,scat}$) can be assigned to the aggregation of unimers into quasi-equilibrium micelles, while the slow process ($\tau_{2,scat}$) is associated with micelle formation/breakup, approaching the final equilibrium state. In principle, the fast process should proceed first with the formation of large numbers of small transient micelles while the unimer concentration is simultaneously reduced to close to the critical micellization concentration (cmc); these transient micelles then grow and fuse to form quasi-equilibrium micelles.

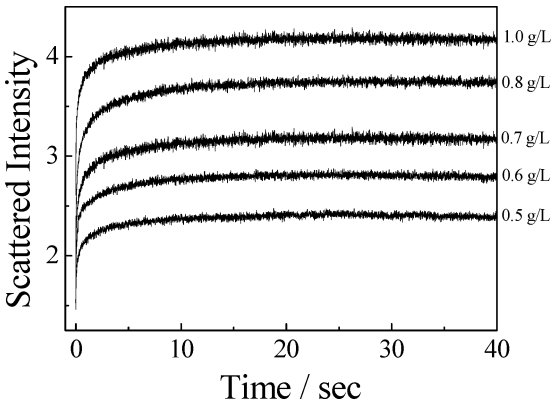

Figure 7. Time dependence of scattered light intensity recorded for various final copolymer concentrations (g/L) obtained after a stopped-flow pH jump from 4.0 to 9.0.

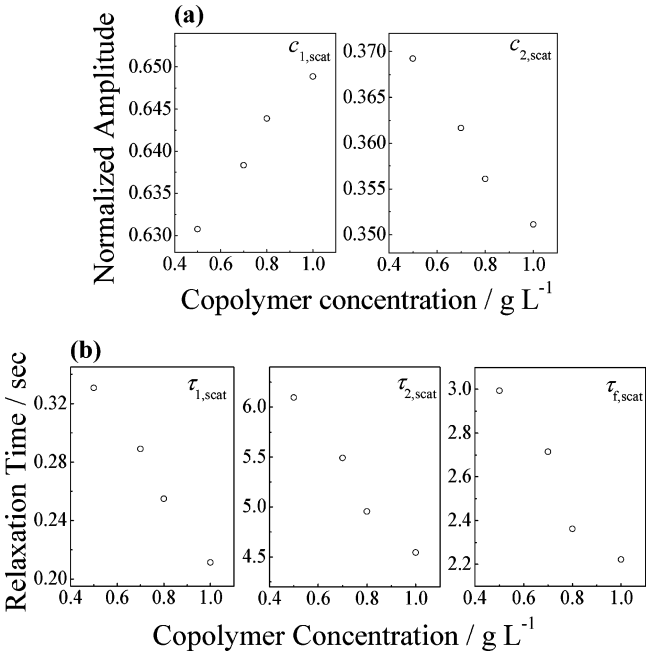

Figure 8. Double exponential fitting results of dynamic traces shown in Figure 7.

Compared to scattered light intensity at 90°, excimer fluorescence is very sensitive to the formation of small aggregates. For the pyrene end-labeled copolymer, even the formation of dimers will give rise to strong excimer emission.[76] Thus, the detected $\tau_{1,fluo}$ by stopped-flow fluorescence on time scales of the order of a few milliseconds must be due to the initial formation of small transient micelles. This should lead to the close proximity of pyrene groups and the appearance of an excimer emission signal. Since evolution of the scattered light intensity does not reveal such a dramatic increase within the initial 10 ms compared to the I_E/I_M ratio, the small transient micelles presumably comprise only a few copolymer chains. We believe that this is the first direct experimental evidence supporting the initial formation of transient micelles during the unimer-to-micelle transition.

Figures 7 and 9 show the time dependence for the scattered light intensity and I_E/I_M ratios after a pH jump from 4.0 to 9.0 at different copolymer concentrations. The corresponding double exponential and triple exponential fitting results are shown in Figures 8 and 10, respectively. According to Figure 10b, $\tau_{1,fluo}$ decreases with increasing copolymer concentration. This is reasonable given that the initial formation of small transient

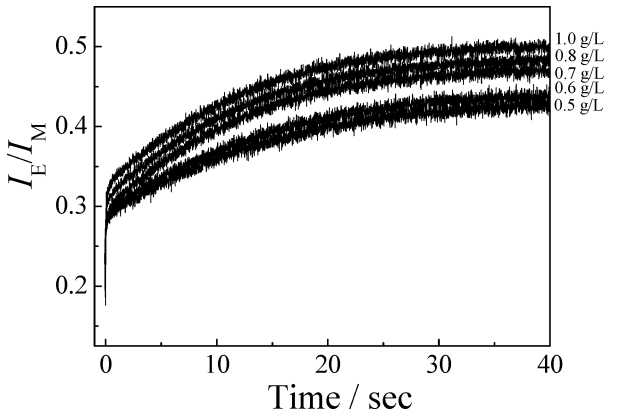

Figure 9. Time dependence of excimer/monomer fluorescence intensity ratios (I_E/I_M) obtained at various final copolymer concentrations (g/L) after a pH jump from 4.0 to 9.0.

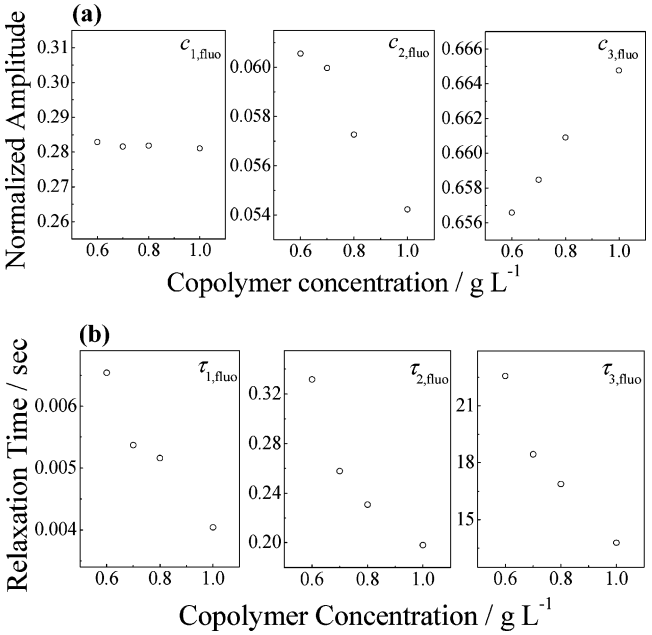

Figure 10. Triple exponential fitting results of dynamic curves shown in Figure 9.

micelles mainly depends on the unimer diffusion rate and the average interchain separation distance. At higher copolymer concentrations, there are more interchain collisions, which favor the subsequent formation of small micelles.

After the initial formation of small transient micelles, Esselink et al. predicted that fusion between transient micelles should dominate over unimer insertion/expulsion to form quasi-equilibrium micelles.[51] This relaxation process can be monitored by both stopped-flow light scattering and fluorescence. The characteristic relaxation times $\tau_{1,scat}$ and $\tau_{2,fluo}$ (Figures 8b, 10b) are of similar magnitude (ranging from 0.2 to 0.35 s) and decrease with increasing copolymer concentrations. This strongly suggests that relaxation from initially formed transient micelles to quasi-equilibrium micelles mainly proceeds via micelle fusion/fission.

For relaxation from quasi-equilibrium micelles to the final equilibrium micelles, the copolymer concentration dependence of $\tau_{2,scat}$ and $\tau_{3,fluo}$ is also shown in Figure 8b and 10b, respectively. Both parameters decrease with increasing copolymer concentration, suggesting that the micelle fusion/fission mechanism dominates instead of unimer insertion/expulsion.[48,51,77] This is probably due to that at pH ≥ 9.0, the coronal PDMA blocks have less hydrophilic character since they are completely deprotonated.

It is also clear that $\tau_{3,fluo}$ is systematically larger than $\tau_{2,scat}$ (Table 1, Figures 8b and 10b). Approximately 10−20 s after the pH jump, the scattered light intensity becomes almost constant indicating that the average aggregation number, N_{agg}, of PDEA-core micelles stays almost unchanged,[55] while the I_E/I_M ratio continues to gradually increase (Figure 6). This suggests that, during the latter stages of micellization, that is, relaxation from quasi-equilibrium micelles to the final equilibrium micelles, structural rearrangement of chains, at least involving the motion of chain ends, within the micelle cores occurs although N_{agg} remains almost constant. This leads to more compact core packing and thus to a further increase in the I_E/I_M ratio.

Conclusions

The pH-induced micellization kinetics of a pyrene end-labeled diblock copolymer, poly(2-(diethylamino)ethyl methacrylate)-*b*-poly(2-(dimethylamino) ethyl methacrylate) (*Py*-PDEA-*b*-PDMA), was investigated using a combination of stopped-flow light-scattering and fluorescence techniques. After a pH jump from 4.0 to the final pH range of 6.0−7.6, scattered intensity remains almost constant with time, while I_E/I_M ratios decrease gradually with time, with the final values being much larger than those observed at a final pH of 5.0. This indicates weak aggregation of copolymer chains because of the hydrophobic association of pyrene end groups. However, if the final pH was 8.0, both the scattered light intensity and I_E/I_M increase significantly with time, indicating the formation of hydrated micelles.

The time dependence of the scattered light intensity and the I_E/I_M ratio obtained for a pH jump from 4.0 to ≥9.0 was determined and the fitting results were compared to each other. For the first time, we obtained direct evidence supporting the initial formation of small transient micelles during the pH-induced unimer-to-micelle transition. In the final stage of micellization, that is, relaxation from quasi-equilibrium micelles to final equilibrium micelles, we observed structural rearrangement of chains within the micelle cores and their further compaction during its formation by stopped-flow fluorescence technique.

In summary, a combination of stopped-flow light scattering and fluorescence is shown to be quite powerful for monitoring hitherto undetected kinetic events during the micellar self-assembly of pH-responsive block copolymers in aqueous solution.

Acknowledgment. This work was financially supported by an Outstanding Youth Fund (50425310) and research grants (20534020 and 20674079) from the National Natural Scientific Foundation of China (NNSFC), the "Bai Ren" Project and Special Grant (KJCX2-SW-H14) of the Chinese Academy of Sciences, and the Program for Changjiang Scholars and Innovative Research Team in University (PCSIRT).

References and Notes

(1) Alarcon, C. D. H.; Pennadam, S.; Alexander, C. *Chem. Soc. Rev.* **2005**, *34*, 276−285.

(2) Cunliffe, D.; Alarcon, C. D.; Peters, V.; Smith, J. R.; Alexander, C. *Langmuir* **2003**, *19*, 2888−2899.

(3) Hoffmann, J.; Plotner, M.; Kuckling, D.; Fischer, W. J. *Sens. Actuators, A-Phys.* **1999**, *77*, 139−144.

(4) Ista, L. K.; Lopez, G. P. *J. Ind. Microbiol. Biotechnol.* **1998**, *20*, 121−125.

(5) Kim, S. J.; Park, S. J.; Lee, S. M.; Lee, Y. M.; Kim, H. C.; Kim, S. I. *J. Appl. Polym. Sci.* **2003**, *89*, 890−894.

(6) Liu, S. Y.; Armes, S. P. *Langmuir* **2003**, *19*, 4432−4438.
(7) Nandkumar, M. A.; Yamato, M.; Kushida, A.; Konno, C.; Hirose, M.; Kikuchi, A.; Okano, T. *Biomaterials* **2002**, *23*, 1121−1130.
(8) Raula, J.; Shan, J.; Nuopponen, M.; Niskanen, A.; Jiang, H.; Kauppinen, E. I.; Tenhu, H. *Langmuir* **2003**, *19*, 3499−3504.
(9) Riess, G. *Prog. Polym. Sci.* **2003**, *28*, 1107−1170.
(10) Rodriguez-Hernandez, J.; Checot, F.; Gnanou, Y.; Lecommandoux, S. *Prog. Polym. Sci.* **2005**, *30*, 691−724.
(11) Schild, H. G. *Prog. Polym. Sci.* **1992**, *17*, 163−249.
(12) Urry, D. W. *Biopolymers* **1998**, *47*, 167−178.
(13) Yamato, M.; Utsumi, M.; Kushida, A.; Konno, C.; Kikuchi, A.; Okano, T. *Tissue Eng.* **2001**, *7*, 473−480.
(14) Colfen, H. *Macromol. Rapid Commun.* **2001**, *22*, 219−252.
(15) Butun, V.; Billingham, N. C.; Armes, S. P. *J. Am. Chem. Soc.* **1998**, *120*, 11818−11819.
(16) Rodriguez-Hernandez, J.; Lecommandoux, S. *J. Am. Chem. Soc.* **2005**, *127*, 2026−2027.
(17) Maeda, Y.; Mochiduki, H.; Ikeda, I. *Macromol. Rapid Commun.* **2004**, *25*, 1330−1334.
(18) Arotcarena, M.; Heise, B.; Ishaya, S.; Laschewsky, A. *J. Am. Chem. Soc.* **2002**, *124*, 3787−3793.
(19) Virtanen, J.; Arotcarena, M.; Heise, B.; Ishaya, S.; Laschewsky, A.; Tenhu, H. *Langmuir* **2002**, *18*, 5360−5365.
(20) Andre, X.; Zhang, M. F.; Muller, A. H. E. *Macromol. Rapid Commun.* **2005**, *26*, 558−563.
(21) Schilli, C. M.; Zhang, M. F.; Rizzardo, E.; Thang, S. H.; Chong, Y. K.; Edwards, K.; Karlsson, G.; Muller, A. H. E. *Macromolecules* **2004**, *37*, 7861−7866.
(22) Gil, E. S.; Hudson, S. A. *Prog. Polym. Sci.* **2004**, *29*, 1173−1222.
(23) Alarcon, C. D. H.; Pennadam, S.; Alexander, C. *Chem. Soc. Rev.* **2005**, *34*, 276−285.
(24) Dai, S.; Ravi, P.; Tam, K. C.; Mao, B. W.; Gang, L. H. *Langmuir* **2003**, *19*, 5175−5177.
(25) Gan, L. H.; Ravi, P.; Mao, B. W.; Tam, K. C. *J. Polym. Sci., Part A: Polym. Chem.* **2003**, *41*, 2688−2695.
(26) Butun, V.; Liu, S.; Weaver, J. V. M.; Bories-Azeau, X.; Cai, Y.; Armes, S. P. *React. Funct. Polym.* **2006**, *66*, 157−165.
(27) Liu, S. Y.; Armes, S. P. *Angew. Chem., Int. Ed.* **2002**, *41*, 1413−1416.
(28) Sumerlin, B. S.; Lowe, A. B.; Thomas, D. B.; Convertine, A. J.; Donovan, M. S.; McCormick, C. L. *J. Polym. Sci., Part A: Polym. Chem.* **2004**, *42*, 1724−1734.
(29) Poe, G. D.; McCormick, C. L. *J. Polym. Sci., Part A: Polym. Chem.* **2004**, *42*, 2520−2533.
(30) Gohy, J. F. *Adv. Polym. Sci.* **2005**, *190*, 65−136.
(31) Riess, G. *Prog. Polym. Sci.* **2003**, *28*, 1107−1170.
(32) Chen, G. P.; Ito, Y.; Imanishi, Y. *Macromolecules* **1997**, *30*, 7001−7003.
(33) Liu, S. Y.; Billingham, N. C.; Armes, S. P. *Angew. Chem., Int. Ed.* **2001**, *40*, 2328−2331.
(34) Zhang, W. Q.; Shi, L. Q.; Ma, R. J.; An, Y. L.; Xu, Y. L.; Wu, K. *Macromolecules* **2005**, *38*, 8850−8852.
(35) Martin, T. J.; Prochazka, K.; Munk, P.; Webber, S. E. *Macromolecules* **1996**, *29*, 6071−6073.
(36) Webber, G. B.; Wanless, E. J.; Butun, V.; Armes, S. P.; Biggs, S. *Nano Lett.* **2002**, *2*, 1307−1313.
(37) Vamvakaki, M.; Unali, G. F.; Butun, V.; Boucher, S.; Robinson, K. L.; Billingham, N. C.; Armes, S. P. *Macromolecules* **2001**, *34*, 6839−6841.
(38) Vamvakaki, M.; Billingham, N. C.; Armes, S. P. *Macromolecules* **1999**, *32*, 2088−2090.
(39) Lee, A. S.; Gast, A. P.; Butun, V.; Armes, S. P. *Macromolecules* **1999**, *32*, 4302−4310.
(40) Lee, A. S.; Butun, V.; Vamvakaki, M.; Armes, S. P.; Pople, J. A.; Gast, A. P. *Macromolecules* **2002**, *35*, 8540−8551.
(41) Butun, V.; Billingham, N. C.; Armes, S. P. *J. Am. Chem. Soc.* **1998**, *120*, 11818−11819.
(42) Butun, V.; Billingham, N. C.; Armes, S. P. *Chem. Commun.* **1997**, 671−672.
(43) Butun, V.; Armes, S. P.; Billingham, N. C. *Polymer* **2001**, *42*, 5993−6008.
(44) Butun, V.; Armes, S. P.; Billingham, N. C. *Macromolecules* **2001**, *34*, 1148−1159.
(45) Banez, M. V. D.; Robinson, K. L.; Butun, V.; Armes, S. P. *Polymer* **2001**, *42*, 29−37.
(46) Weaver, J. V. M.; Armes, S. P.; Butun, V. *Chem. Commun.* **2002**, 2122−2123.
(47) Liu, S. Y.; Billingham, N. C.; Armes, S. P. *Angew. Chem., Int. Ed.* **2001**, *40*, 2328−2331.
(48) Halperin, A.; Alexander, S. *Macromolecules* **1989**, *22*, 2403−2412.
(49) Wang, Y. M.; Mattice, W. L.; Napper, D. H. *Langmuir* **1993**, *9*, 66−70.
(50) Esselink, F. J.; Dormidontova, E. E.; Hadziioannou, G. *Macromolecules* **1998**, *31*, 4873−4878.
(51) Esselink, F. J.; Dormidontova, E.; Hadziioannou, G. *Macromolecules* **1998**, *31*, 2925−2932.
(52) Dormidontova, E. E. *Macromolecules* **1999**, *32*, 7630−7644.
(53) Nyrkova, I. A.; Semenov, A. N. *Macromol. Theory Simul.* **2005**, *14*, 569−585.
(54) Nyrkova, I. A.; Semenov, A. N. *Faraday Discuss.* **2005**, *128*, 113−127.
(55) Zhu, Z. Y.; Armes, S. P.; Liu, S. Y. *Macromolecules* **2005**, *38*, 9803−9812.
(56) Wang, D.; Yin, J.; Zhu, Z. Y.; Ge, Z. S.; Liu, H. W.; Armes, S. P.; Liu, S. Y. *Macromolecules* **2006**, *39*, 7378−7385.
(57) Kalyanasundaram, K.; Thomas, J. K. *J. Am. Chem. Soc.* **1977**, *99*, 2039−2044.
(58) Chen, W.; Durning, C. J.; Turro, N. J. *Macromolecules* **1999**, *32*, 4151−4153.
(59) Picarra, S.; Relogio, P.; Afonso, C. A. M.; Martinho, J. M. G.; Farinha, J. P. S. *Macromolecules* **2003**, *36*, 8119−8129.
(60) Picarra, S.; Relogio, P.; Afonso, C. A. M.; Martinho, J. M. G.; Farinha, J. P. S. *Macromolecules* **2004**, *37*, 1670−1670.
(61) Picarra, S.; Duhamel, J.; Fedorov, A.; Martinho, J. M. G. *J. Phys. Chem. B* **2004**, *108*, 12009−12015.
(62) Winnik, F. M. *Macromolecules* **1990**, *23*, 233−242.
(63) Farinha, J. P. S.; Picarra, S.; Miesel, K.; Martinho, J. M. G. *J. Phys. Chem. B* **2001**, *105*, 10536−10545.
(64) Picarra, S.; Gomes, P. T.; Martinho, J. M. G. *Macromolecules* **2000**, *33*, 3947−3950.
(65) Winnik, F. M. *Langmuir* **1990**, *6*, 522−524.
(66) Picarra, S.; Pereira, E. J. N.; Bodunov, E. N.; Martinho, J. M. G. *Macromolecules* **2002**, *35*, 6397−6403.
(67) Winnik, F. M. *Macromolecules* **1990**, *23*, 1647−1649.
(68) Picarra, S.; Martinho, J. M. G. *Macromolecules* **2001**, *34*, 53−58.
(69) Webber, G. B.; Wanless, E. J.; Armes, S. P.; Tang, Y. Q.; Li, Y. T.; Biggs, S. *Adv. Mater.* **2004**, *16*, 1794−1798.
(70) Zhu, Z. Y.; Gonzalez, Y. I.; Xu, H. X.; Kaler, E. W.; Liu, S. Y. *Langmuir* **2006**, *22*, 949−955.
(71) Liu, S. Y.; Weaver, J. V. M.; Tang, Y. Q.; Billingham, N. C.; Armes, S. P.; Tribe, K. *Macromolecules* **2002**, *35*, 6121−6131.
(72) Plamper, F. A.; Becker, H.; Lanzendorfer, M.; Patel, M.; Wittemann, A.; Ballauf, M.; Muller, A. H. E. *Macromol. Chem. Phys.* **2005**, *206*, 1813−1825.
(73) Vamvakaki, M.; Palioura, D.; Spyros, A.; Armes, S. P.; Anastasiadis, S. H. *Macromolecules* **2006**, *39*, 5106−5112.
(74) Snare, M. J.; Thistlewaite, P. J.; Ghiggino, K. P. *J. Am. Chem. Soc.* **1983**, *105*, 3328−3332.
(75) Zagrobelny, J.; Betts, T. A.; Bright, F. V. *J. Am. Chem. Soc.* **1992**, *114*, 5249−5257.
(76) Winnik, F. M. *Chem. Rev.* **1993**, *93*, 587−614.
(77) Haliloglu, T.; Bahar, I.; Erman, B.; Mattice, W. L. *Macromolecules* **1996**, *29*, 4764−4771.